

Supplementary Materials: Photophysics of BODIPY Dyes as Readily Designable Photosensitisers in Light-Driven Proton Reduction

**Laura Dura, Maria Wächtler, Stephan Kupfer, Joachim Kübel, Johannes Ahrens, Sebastian Höfler,
Martin Bröring, Benjamin Dietzek, Torsten Beweries**

S2	Volumetric curves (as measured) and Hg experiments
S3	Stationary emission spectra
S5	Stern Volmer experiments
S8	Transient absorption spectra
S11	Quantum chemical calculations
S21	Analysis of transient absorption data
S23	ESI-MS data

Volumetric Curves

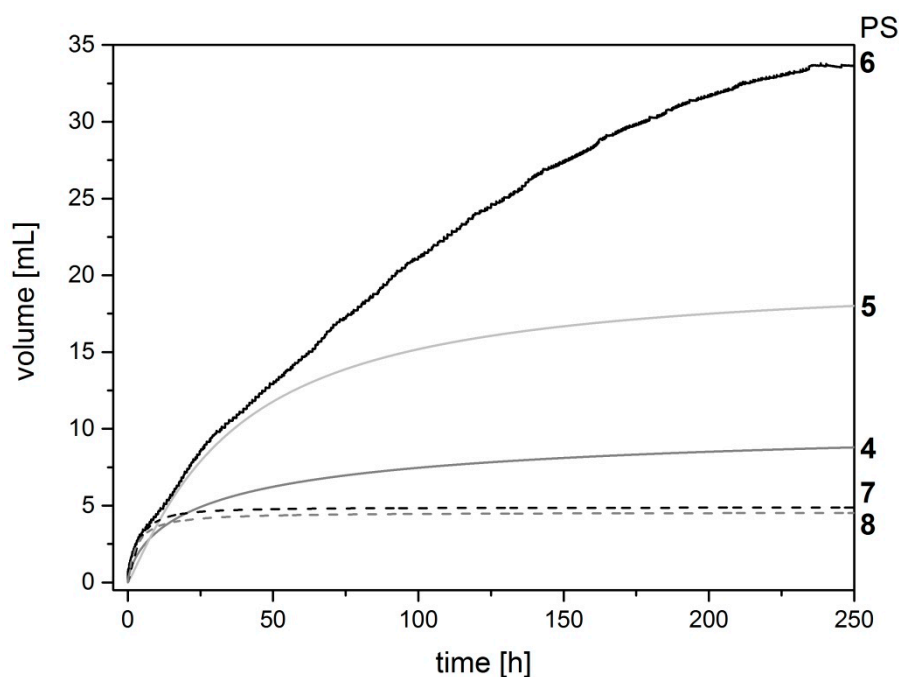


Figure S1. Volumetric curves (original data) as measured using multicomponent catalyst systems sensitized by 4–8 containing 10 mL of a 1 mM solution of the PS in THF, 1 mL of a 1 mM solution of $[\text{PdCl}_2(\text{PPh}_3)]_2$ in THF, 3 mL water, and 8 mL TEA.

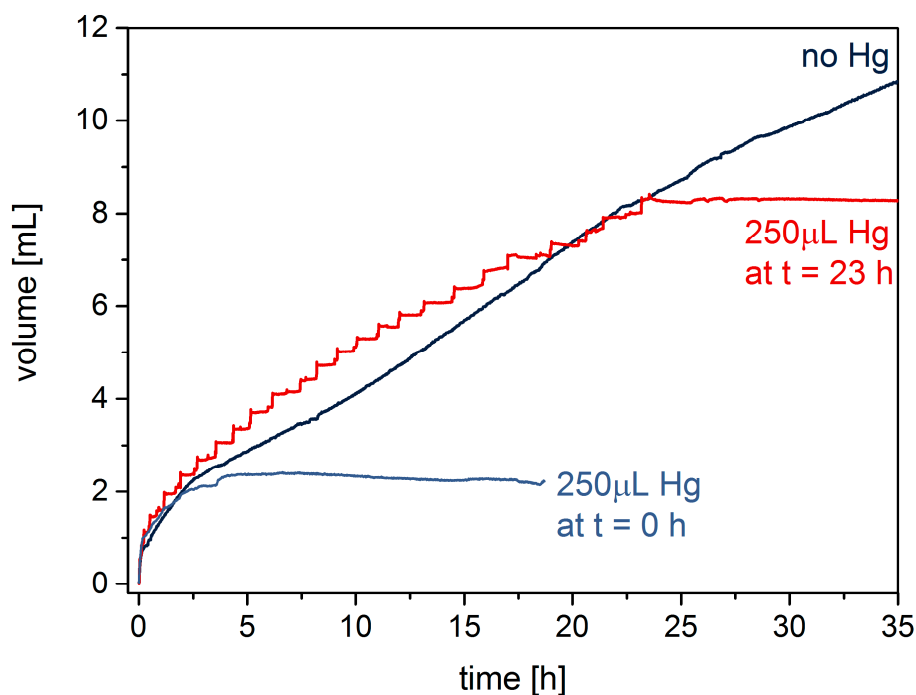


Figure S2. Comparison of volumetric curves (original data) as measured using multicomponent catalyst systems containing 10 mL of a 1 mM solution of in THF, 1 mL of a 1 mM solution of $[\text{PdCl}_2(\text{PPh}_3)]_2$ in THF, 3 mL water, 8 mL TEA, and 250 μL Hg.

Stationary Emission Spectra

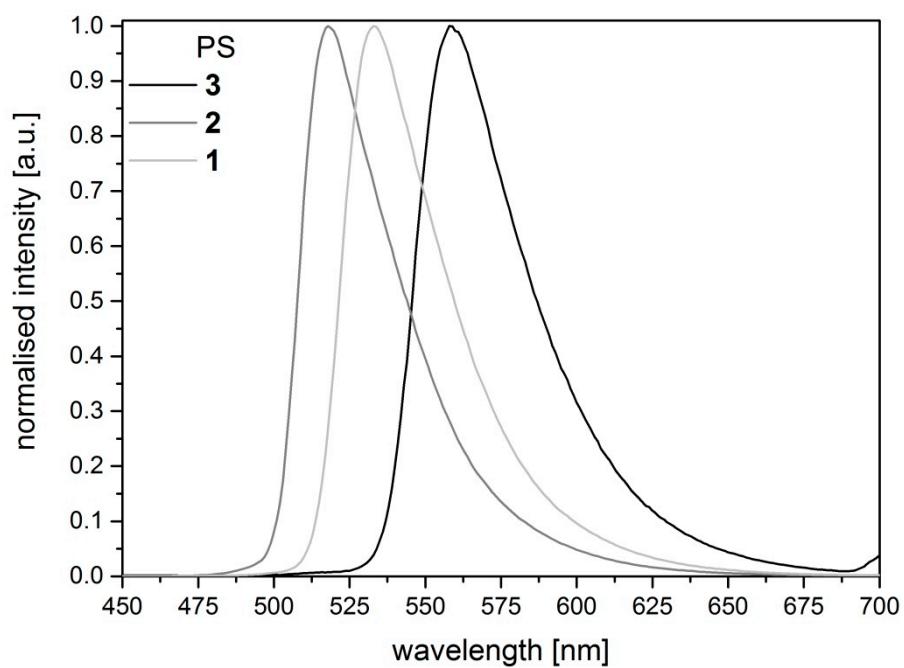


Figure S3. Normalised emission spectra of pure BODIPY dyes 1–3 measured in THF, $c = 5 \times 10^{-5}$ M, $\lambda_{exc} = 350$ nm.

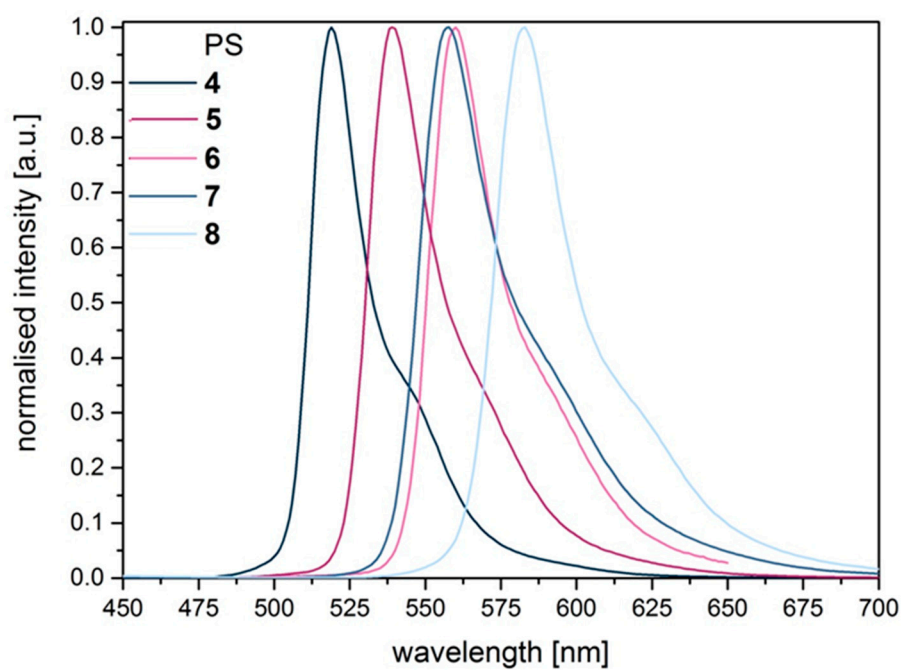


Figure S4. Normalised emission spectra of pure BODIPY dyes 4–8 measured in THF, $c = 5 \times 10^{-5}$ M, $\lambda_{exc} = 350$ nm.

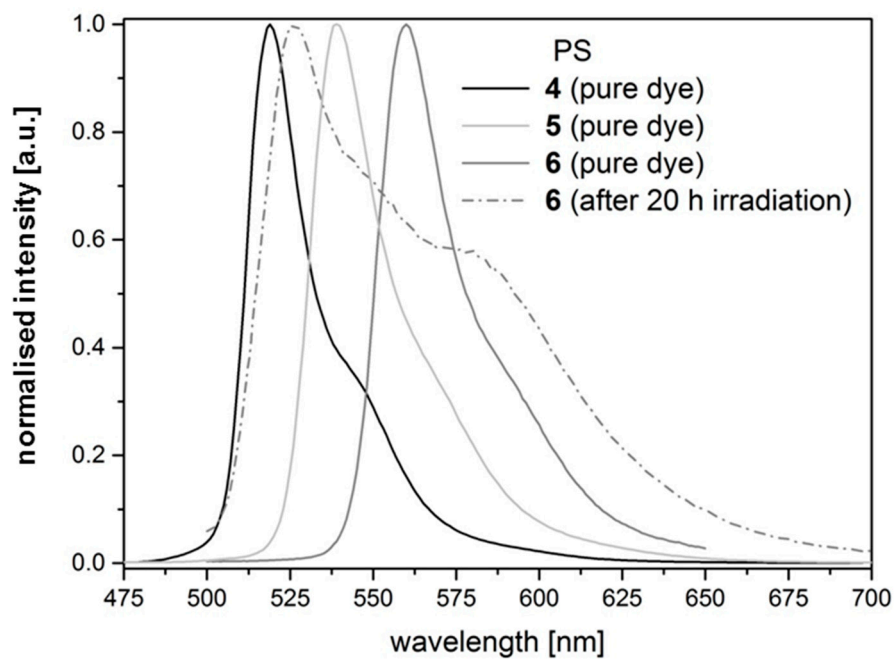


Figure S5. Emission spectra of pure BODIPY dyes **4–6** and a **6**-sensitized multicomponent catalyst system after 20 h of irradiation measured in THF, $c = 5 \times 10^{-5}$ M, $\lambda_{exc} = 350$ nm.

Stern-Volmer Experiments

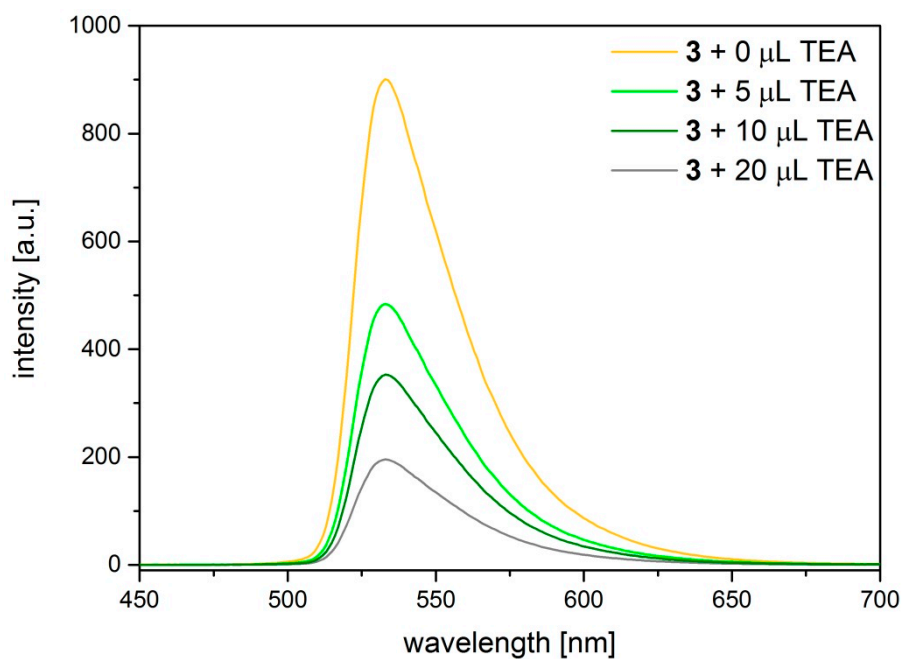


Figure S6. Example for stationary Stern-Volmer experiments with *meso*-methyl substituted BODIPY dyes. Fluorescence quenching with triethylamine (TEA) was observed on a 5×10^{-5} M solution of **3** in THF.

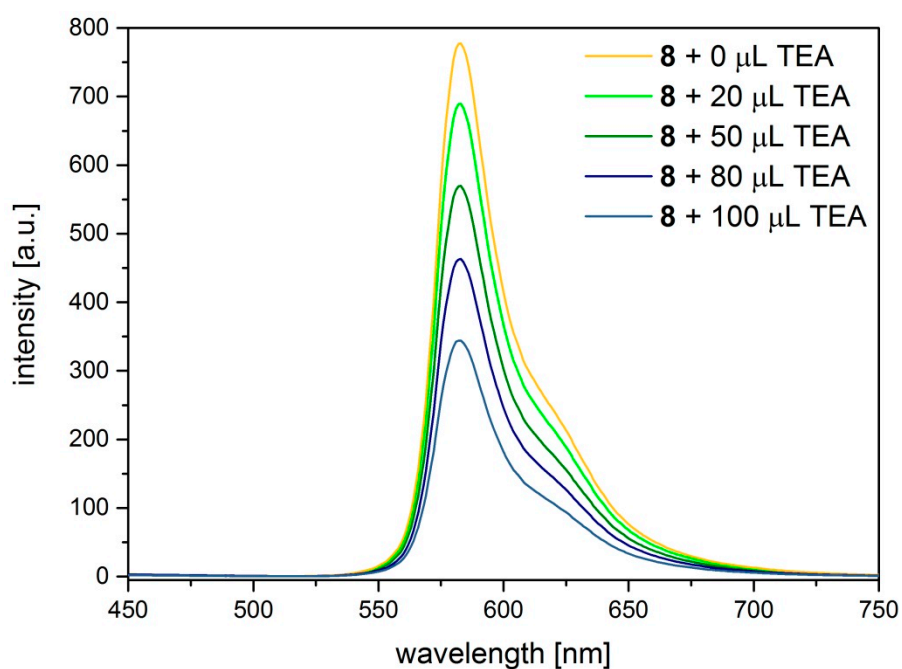


Figure S7. Example for stationary Stern-Volmer experiments with *meso*-mesityl substituted BODIPY dyes. Fluorescence quenching with triethylamine (TEA) was observed on a 5×10^{-5} M solution of **8** in THF.

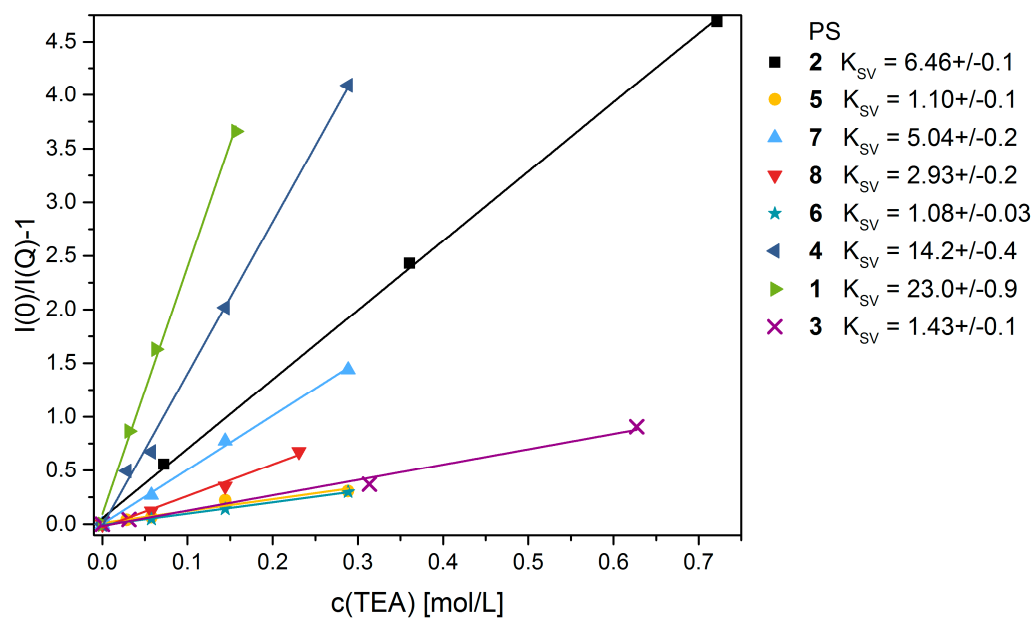


Figure S8. Stern-Volmer plots of fluorescence quenching experiments on BODIPY dyes with TEA.

Stern–Volmer Kinetics

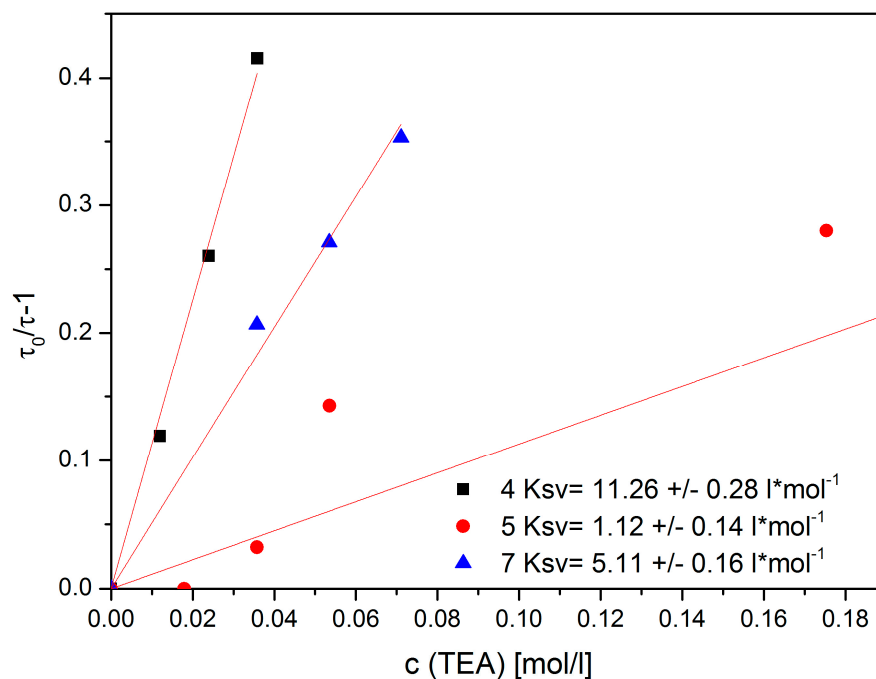


Figure S9. Stern–Volmer Plots from emission lifetime quenching with TEA.

Table S1. Lifetimes and parameters for the Stern–Volmer Plots.

4			5			7		
c(TEA)	τ_{em} / ns^*	$\tau_0/\tau_{em}-1$	c(TEA)	τ_{em} / ns^*	$\tau_0/\tau_{em}-1$	c(TEA)	τ_{em} / ns^*	$\tau_0/\tau_{em}-1$
0	4.62	0	0	0.32	0	0	5.02	0
0.01198	4.11	0.12	0.01793	0.32	0	0.03571	4.16	0.21
0.02393	3.65	0.26	0.03577	0.31	0.03	0.05344	3.95	0.27
0.03583	3.25	0.42	0.05352	0.28	0.14	0.07108	3.71	0.35
			0.17536	0.25	0.28			
			0.34239	0.24	0.33			

*+/- 1%

ns Time-Resolved Transient Absorption Spectra and Kinetics

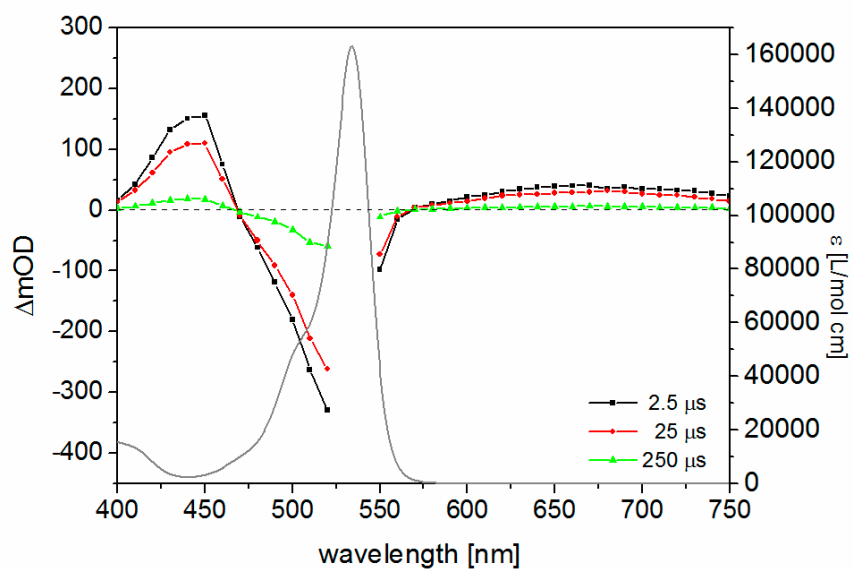


Figure S10. Transient absorption spectra at chosen delay times (black, red, green) upon excitation with the pump pulse centred at 535 nm and stationary absorption spectrum (grey) of 6 in THF.

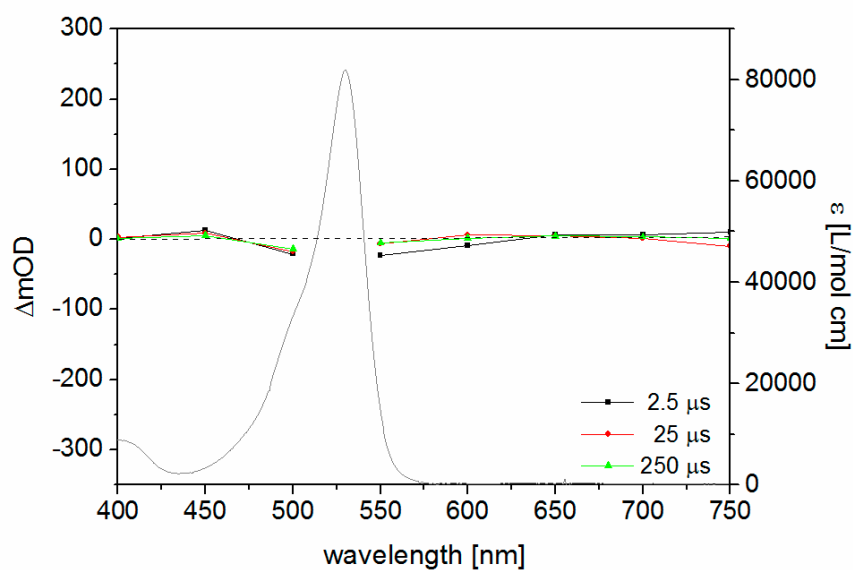


Figure S11. Transient absorption spectra at chosen delay times (black, red, green) upon excitation with the pump pulse centred at 530 nm and stationary absorption spectrum (grey) of 7 in THF.

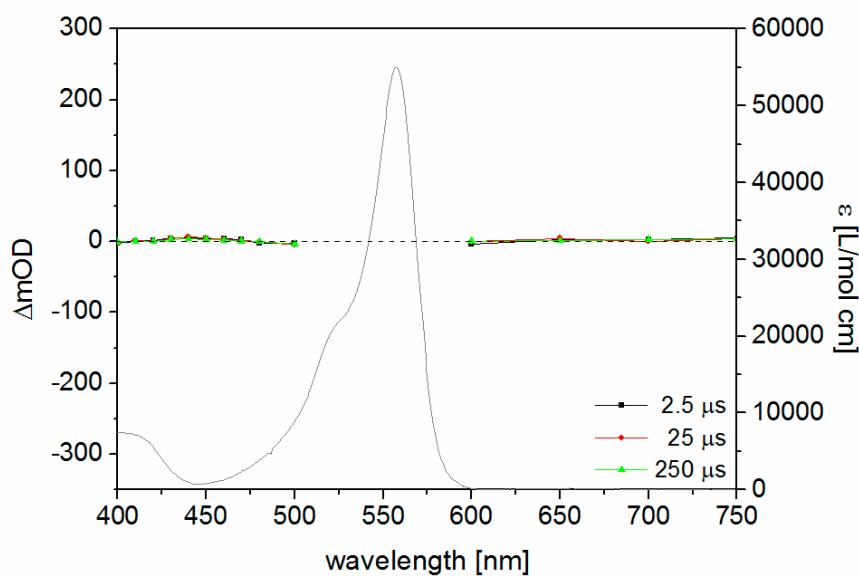


Figure S12. Transient absorption spectra at chosen delay times (black, red, green) upon excitation with the pump pulse centred at 560 nm and stationary absorption spectrum (grey) of **8** in THF.

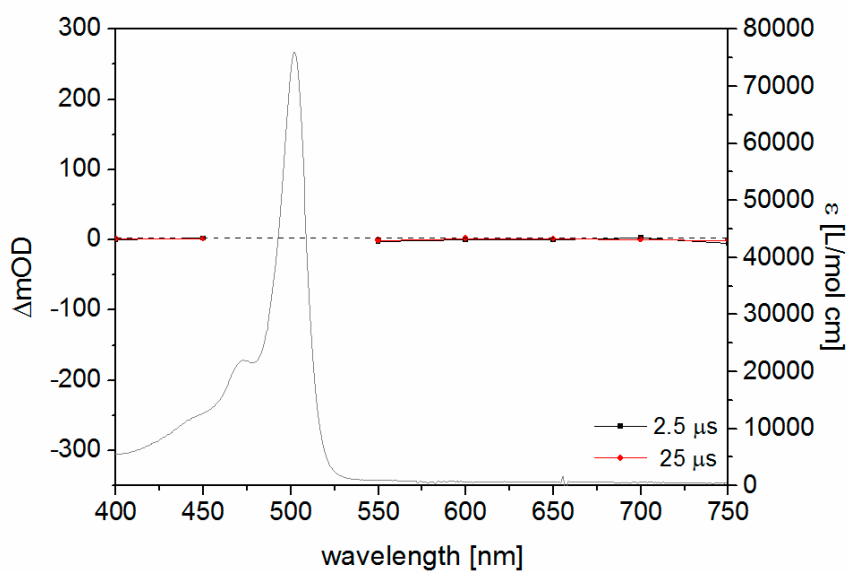


Figure S13. Transient absorption spectra at chosen delay times (black, red, green) upon excitation with the pump pulse centred at 500 nm and stationary absorption spectrum (grey) of **4** in THF.

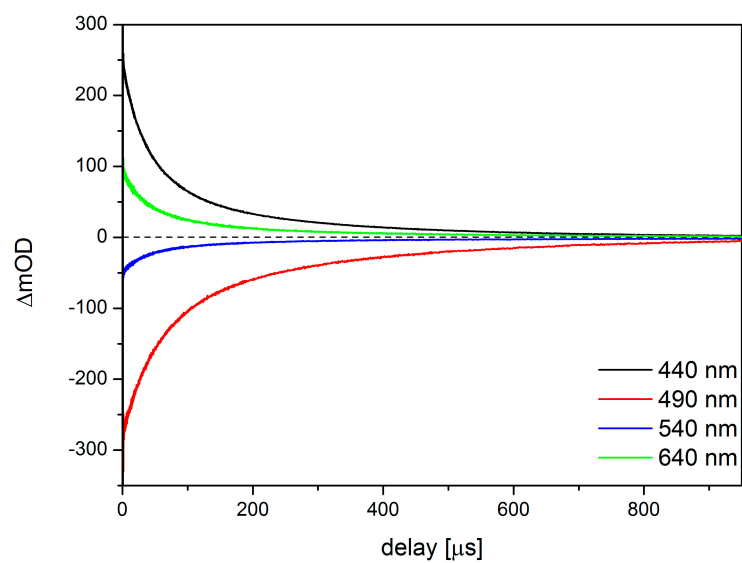


Figure S14. ns- transient absorption decay kinetics of the long-lived triplet state of **5** at chosen probe wavelengths.

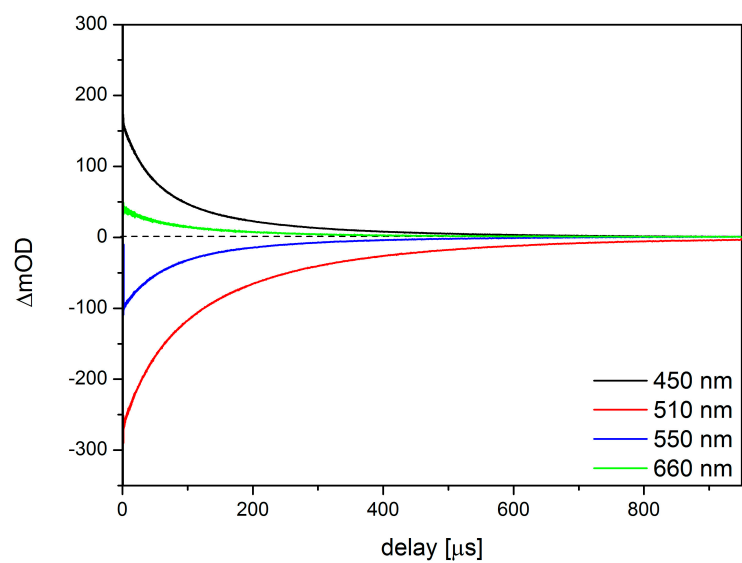


Figure S15. ns- transient absorption decay kinetics of the long-lived triplet state of **6** at chosen probe wavelengths.

Quantum Chemical Evaluation

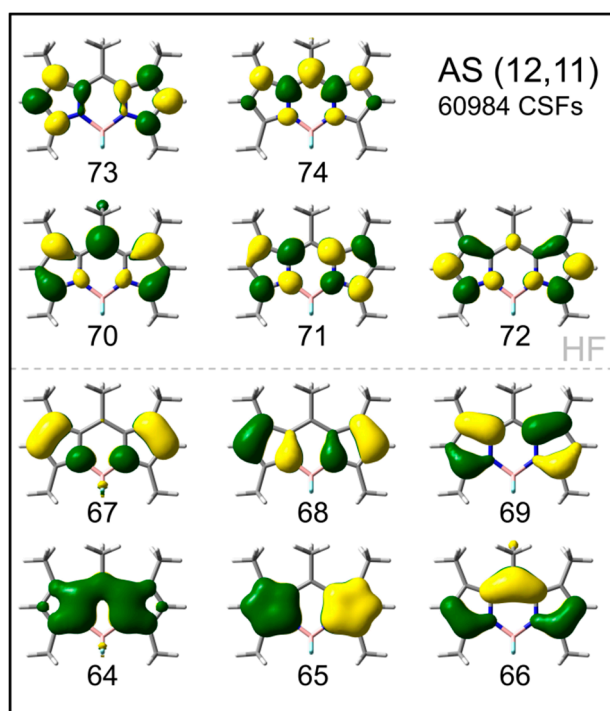


Figure S16. MOs of the AS (12,11), comprising the entire $\pi\pi^*$ system of **2**, used in the MS-CASPT2//CASSCF reference calculations. Grey line indicates to the occupation of the MOs within the Hartree-Fock wavefunction.

Table S2. Leading transitions, excitation energies (in eV), wavelengths (in nm), and oscillator strengths obtained by MS-CASPT2 (gas phase) and by TDDFT using the PBE0 functional for the low-lying singlet and triplet states of **2**. TDDFT values are given in gas phase and in THF (in parentheses).

MS-CASPT2						TD-PBE0				
	Transition	weight	E^e / eV	λ / nm	f	Transition	weight / %	E^e / eV	λ / nm	f
S ₀	HF	83	-	-	-	-	-	-	-	-
S ₁	69 → 70	57	2.72	456	0.672	69 → 70	95 (99)	3.06	405	0.523
	68 → 70	15						(2.96)	(419)	(0.641)
S ₂	68 → 70	52	3.76	330	0.071	68 → 70	96 (98)	3.65	340	0.062
	69 → 70	13						(3.67)	(338)	(0.058)
	DE	12								
S ₃	67 → 70	58	3.93	315	0.042	67 → 70	99 (99)	3.88	320	0.030
	DE	15						(3.92)	(316)	(0.046)
S ₄	DE	37	4.46	288	0.042	66 → 70	91 (93)	4.94	251	0.138
	66 → 70	26						(4.90)	(253)	(0.194)
	69 → 74	8								
T ₁	69 → 70	82	1.99	623	-	69 → 70	98 (98)	1.55	800	-
								(1.59)	(782)	
T ₂	68 → 70	72	3.23	384	0.004	68 → 70	95 (95)	2.86	434	-
								(2.91)	(426)	
T ₃	67 → 70	67	3.40	365	0.005	67 → 70	86 (83)	2.98	416	-
						66 → 70	8 (11)	(3.04)	(408)	
T ₄	66 → 70	69	3.92	316	0.176	66 → 70	88 (85)	3.44	361	-
	67 → 70	5				67 → 70	8 (12)	(3.45)	(359)	

Table S3. MOs involved in leading transitions of low-lying bright excited singlet state (S₁) and low-lying triplet states (T₁-T₃) within the fully optimized singlet ground state equilibrium structure of **2**.

2 (optimized S₀ geometry)

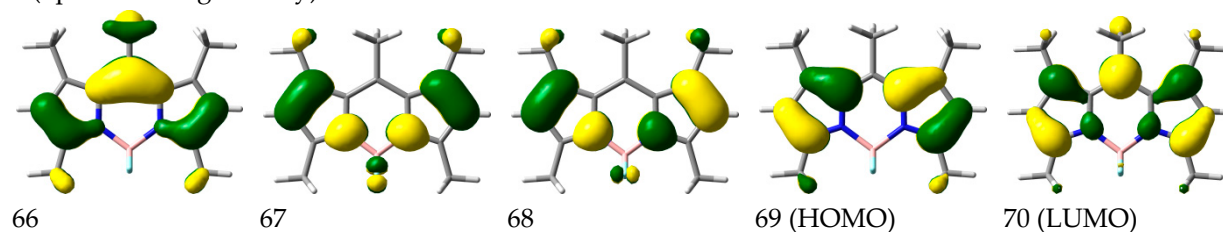
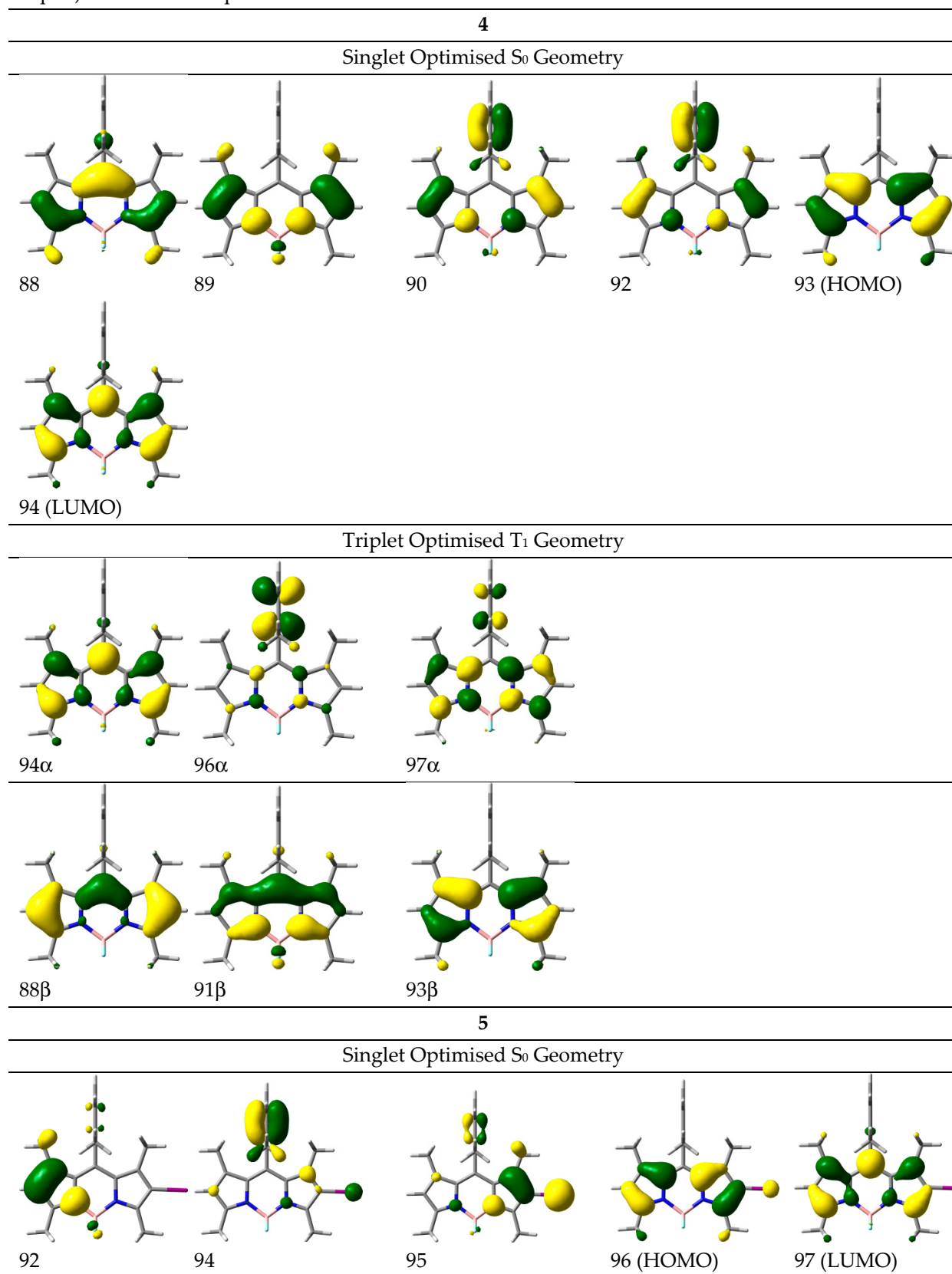
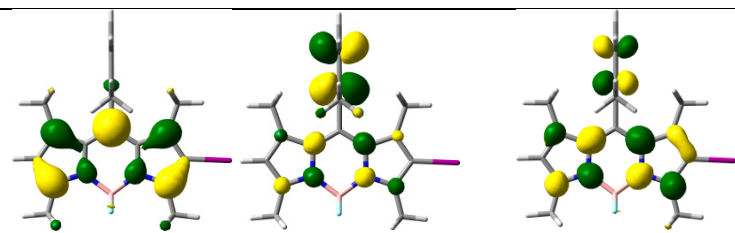
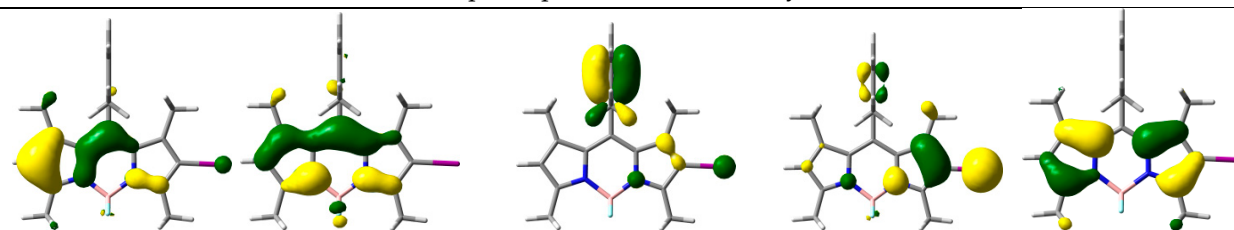


Table S4. Excited and ground state energies of S₀, S₁, T₁, T₂, and T₃ within optimized equilibrium geometries of S₀, S₁ and T₁ for dyes of 4–8. All numbers are given relative to the ground state energy (S₀) in the optimized S₀ structure.

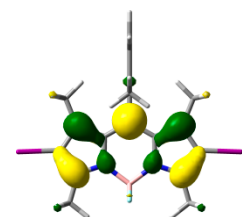
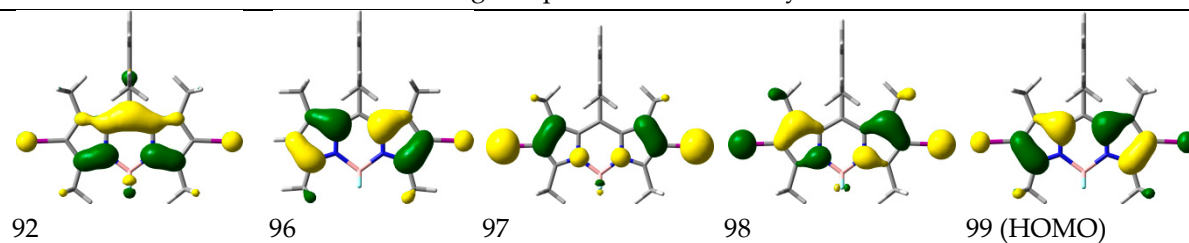
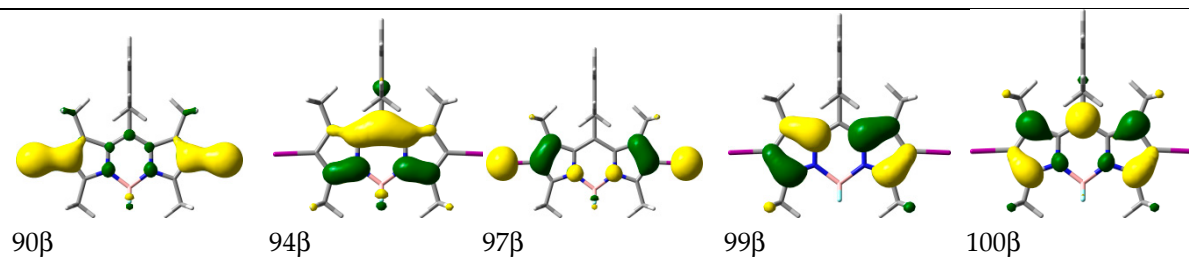
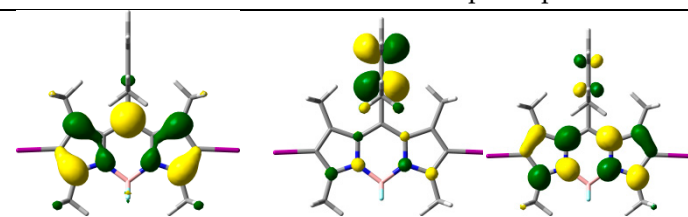
		Equilibrium Geometry														
		4			5			6			7			8		
$E^s(\text{state}) / \text{eV}$	S ₀	S ₀	S ₁	T ₁	S ₀	S ₀	S ₁	T ₁	S ₀	S ₀	S ₁	T ₁	S ₀	S ₀	S ₁	T ₁
	S ₁	0.00	0.04	0.13	0.00	0.04	0.12	0.00	0.05	0.09	0.00	0.04	0.11	0.00	0.04	0.10
	T ₁	2.91	2.71	2.91	2.81	2.63	2.84	2.75	2.59	2.80	2.80	2.62	2.81	2.69	2.52	2.72
	T ₂	1.49	1.41	1.53	1.48	1.45	1.53	1.54	1.56	1.59	1.46	1.41	1.51	1.43	1.40	1.48
	T ₃	2.83	2.88	3.13	2.68	2.66	2.94	2.61	2.57	2.83	2.68	2.69	2.97	2.63	2.63	2.91
	T ₃	3.00	2.99	3.15	2.92	2.94	3.10	2.79	2.73	3.38	2.99	3.00	3.15	2.87	2.88	3.09

Table S5. MOs involved in leading transitions of bright excited singlet states (and low-lying triplet states (T_1 - T_3)) of 4–8 within the S_0 equilibrium structure and bright triplet excited states (triplet-to-triplet) within the T_1 equilibrium structure.

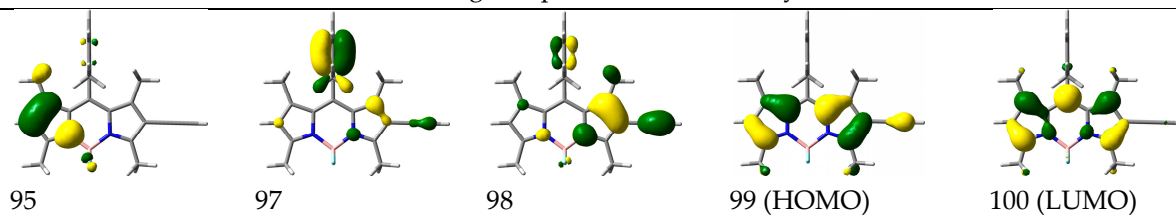
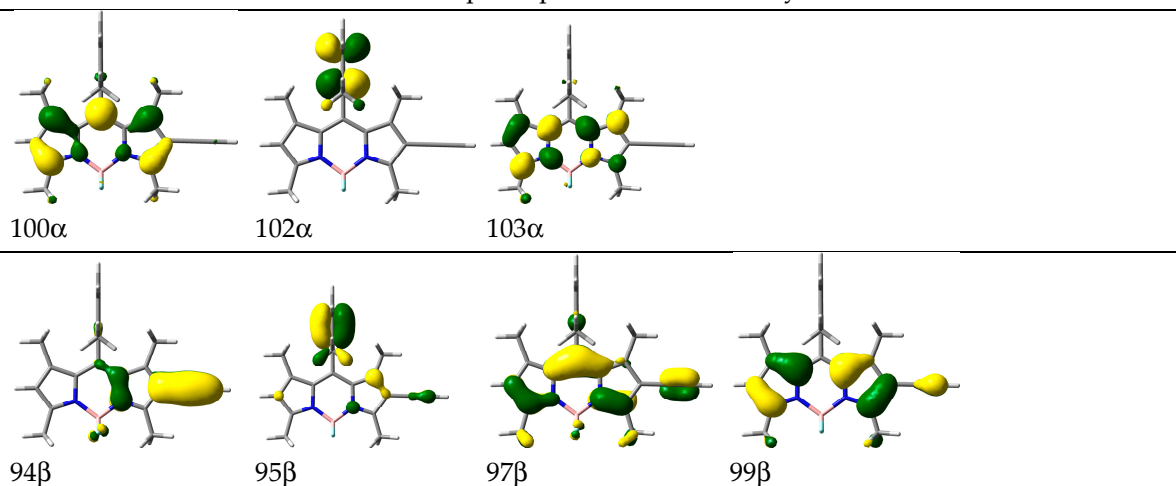


Triplet Optimised T₁ Geometry

6

Singlet Optimised S₀ GeometryTriplet Optimised T₁ Geometry

7

Singlet Optimised S_0 GeometryTriplet Optimised T_1 Geometry

8

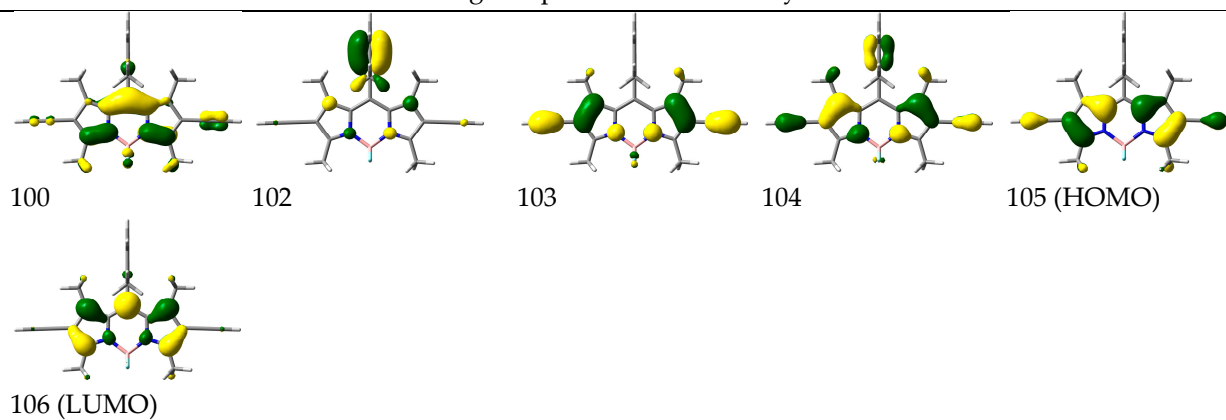
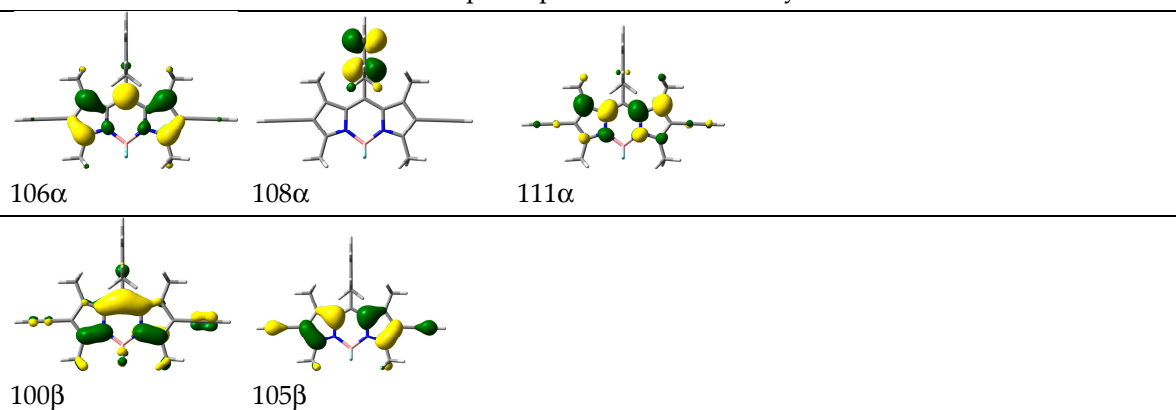
Singlet Optimised S_0 GeometryTriplet Optimised T_1 Geometry

Table S6: Leading transitions, excitation energies (in eV), wavelengths (in nm), oscillator strengths and $\langle s^2 \rangle$ expectation value (spin-contamination) of bright UV-VIS excitations (singlet and triplet)

obtained at the TDDFT level of theory in THF for dyes 4–8. Singlet-to-singlet and triplet-to-triplet excitations were obtained within the respective equilibrium structure.

4						
Singlet Excited States (Optimised S ₀ Geometry)						
state	transition	weight / %	E ^e / eV	λ / nm	f	⟨s ² ⟩
S ₁	93 → 94 LE	99	2.91	427	0.591	-
S ₄	90 → 94 CT	95	3.76	330	0.046	-
S ₅	89 → 94 LE	99	3.85	322	0.043	-
Triplet Excited States (Optimised T ₁ Geometry)						
state	transition	weight / %	E ^e / eV	λ / nm	f	⟨s ² ⟩
T ₂	91β → 93β LE	93	1.60	774	0.036	2.05
T ₅	88β → 93β LE	90	2.22	560	0.067	2.04
T ₈	94α → 96α CT	84	3.27	380	0.195	2.05
	94α → 97α LE	10				
T ₁₀	94α → 97α LE	83	3.54	351	0.168	2.06
	94α → 96α CT	13				
5						
Singlet Excited States (Optimised S ₀ Geometry)						
state	transition	weight / %	E ^e / eV	λ / nm	F	⟨s ² ⟩
S ₁	96 → 97 LE	97	2.81	441	0.616	-
S ₂	95 → 97 LE	93	3.33	373	0.055	-
S ₄	94 → 97 CT	95	3.60	344	0.067	-
S ₅	92 → 97 LE	98	3.73	332	0.049	-
Triplet Excited States (Optimised T ₁ Geometry)						
state	transition	weight / %	E ^e / eV	λ / nm	f	⟨s ² ⟩
T ₃	92β → 96β LE	85	1.58	786	0.026	2.05
T ₅	94β → 96β CT	55	1.99	622	0.068	2.04
	91β → 96β LE	31				
	92β → 96β LE	10				
T ₆	91β → 96β LE	55	2.05	605	0.050	2.04
	94β → 96β CT	34				
	95β → 96β LE	8				
T ₁₀	97α → 100α CT	78	3.28	378	0.284	2.05
	97α → 101α LE	14				

6						
Singlet Excited States (Optimised S ₀ Geometry)						
state	transition	weight / %	E ^e / eV	λ / nm	f	⟨s ² ⟩
S ₁	99 → 100 LE	96	2.75	450	0.692	-
S ₂	98 → 100 LE	93	3.39	366	0.192	-
S ₄	97 → 100 LE	98	3.44	360	0.062	-
S ₅	96 → 100 LE	97	3.53	351	0.036	-
Triplet Excited States (Optimised T ₁ Geometry)						
state	transition	weight / %	E ^e / eV	λ / nm	f	⟨s ² ⟩
T ₃	97β → 99β LE	85	1.42	873	0.015	2.039
	94β → 99β LE	10				
T ₅	94β → 99β LE	84	1.80	691	0.217	2.038
	97β → 99β LE	10				
T ₁₃	100α → 104α CT	51	3.35	370	0.289	2.035
	100α → 105α LE	30				
	90β → 99β LE	12				
T ₁₄	90β → 99β LE	67	3.44	361	0.025	2.064
	98β → 100β LE	12				
	100α → 104α CT	9				
T ₁₆	100α → 105α LE	58	3.54	350	0.116	2.044
	100α → 104α CT	38				
7						
Singlet Excited States (Optimised S ₀ Geometry)						
state	transition	weight / %	E ^e / eV	λ / nm	f	⟨s ² ⟩
S ₁	99 → 100 LE	97	2.80	443	0.640	-
S ₂	98 → 100 LE	92	3.33	372	0.058	-
S ₄	97 → 100 CT	94	3.61	344	0.075	-
S ₅	95 → 100 LE	98	3.74	332	0.049	-
Triplet Excited States (Optimised T ₁ Geometry)						
state	transition	weight / %	E ^e / eV	λ / nm	f	⟨s ² ⟩
T ₃	97β → 99β LE	75	1.64	755	0.034	2.05
	95β → 99β CT	15				
T ₅	94β → 99β LE	79	2.13	583	0.086	2.04
	95β → 99β CT	12				
T ₈	100α → 102α CT	86	3.23	384	0.192	2.05
	100α → 103α LE	8				
T ₁	100α → 103α LE	83	3.50	354	0.190	2.06
	100α → 102α CT	11				

8

Singlet Excited States (Optimised S ₀ Geometry)						
state	transition	weight / %	E ^e / eV	λ / nm	f	⟨s ² ⟩
S ₁	105 → 106 LE	96	2.69	461	0.713	-
S ₂	104 → 106 LE	94	3.24	383	0.071	-
S ₄	103 → 106 LE	97	3.40	365	0.071	-
S ₅	102 → 106 CT	95	3.53	351	0.109	-
Triplet Excited States (Optimised T ₁ Geometry)						
state	transition	weight / %	E ^e / eV	λ / nm	f	⟨s ² ⟩
T ₄	100β → 105β LE	91	2.00	619	0.138	2.04
T ₈	106α → 108α CT	88	3.19	389	0.187	2.05
T ₉	106α → 111α LE	85				
	106α → 108α CT	10	3.47	358	0.221	2.05

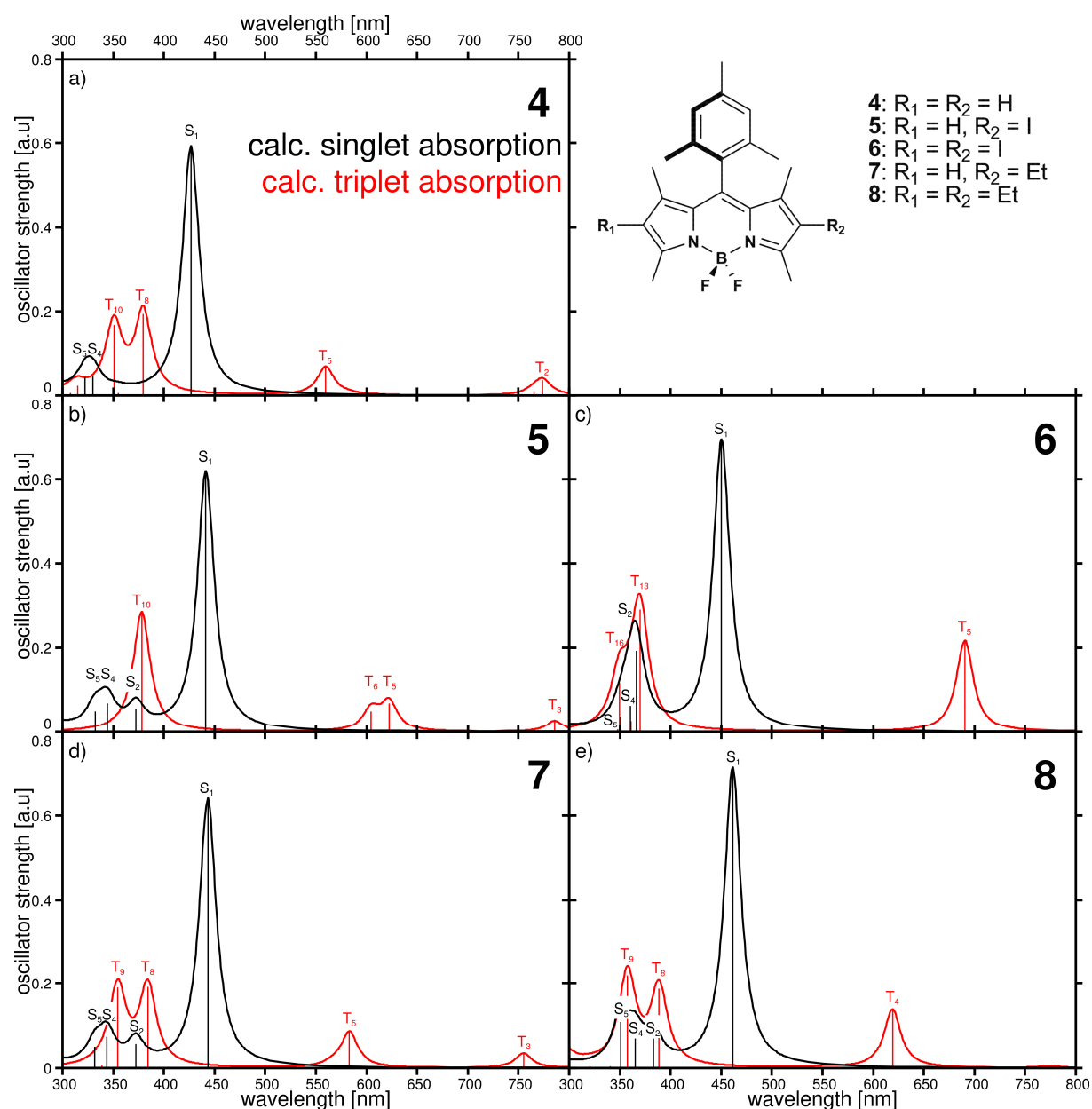


Figure S17. Calculated singlet (in black) and triplet (in red) absorption spectra (THF) of dyes 4–8 within optimised singlet and triplet ground state structures. Triplet absorption spectra are correlated to excited states absorption signals in the transient absorption spectra.

Analysis of fs Transient Absorption Data

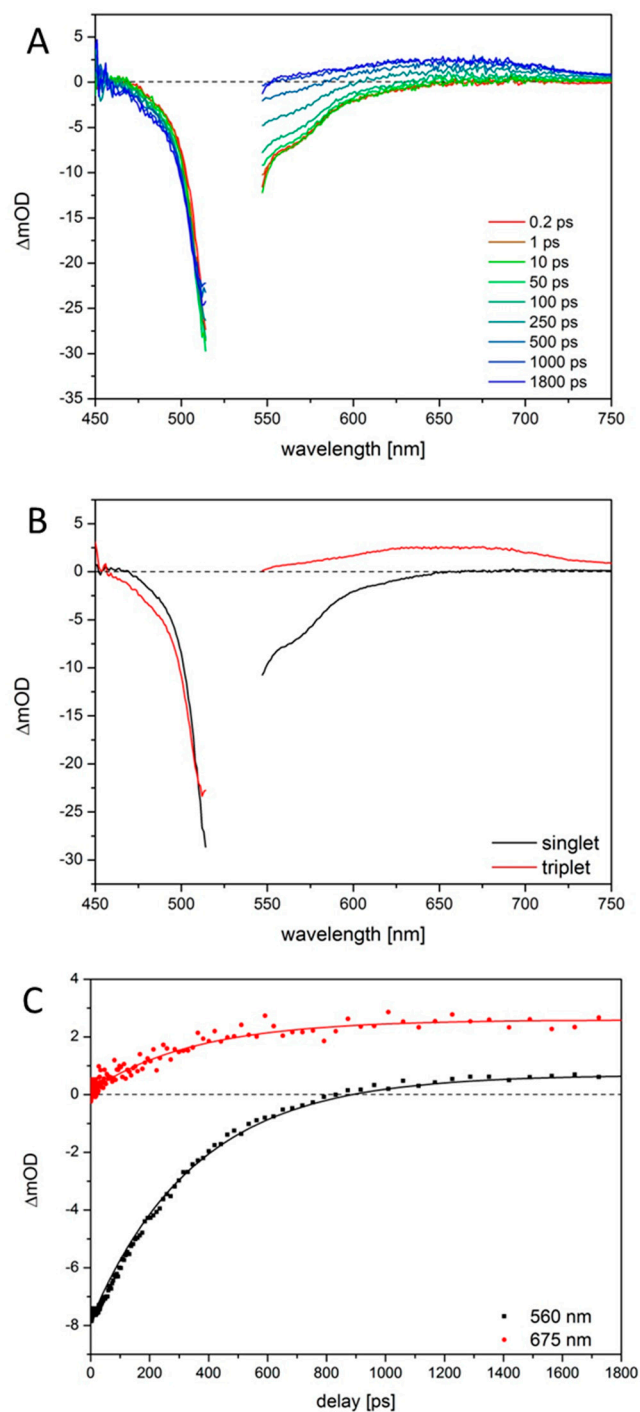


Figure S18. Formation of triplet state in 5: (A) transient spectra at selected delay times, (B) species spectra resulting from the global fit of the data, the spectrum of the initially populated species is assigned to the singlet state and contains mainly contributions of ground-state bleach and stimulated emission, the spectrum of the subsequently with a time constant of 354 ps populated species agrees well with the spectrum of the long-lived species in ns time-resolved measurements, which is assigned to the triplet state (C) kinetic traces at chosen probe wavelengths (line fits). The spectral region around the excitation wavelength (530 nm) was neglected in data evaluation due to a scattered pump.

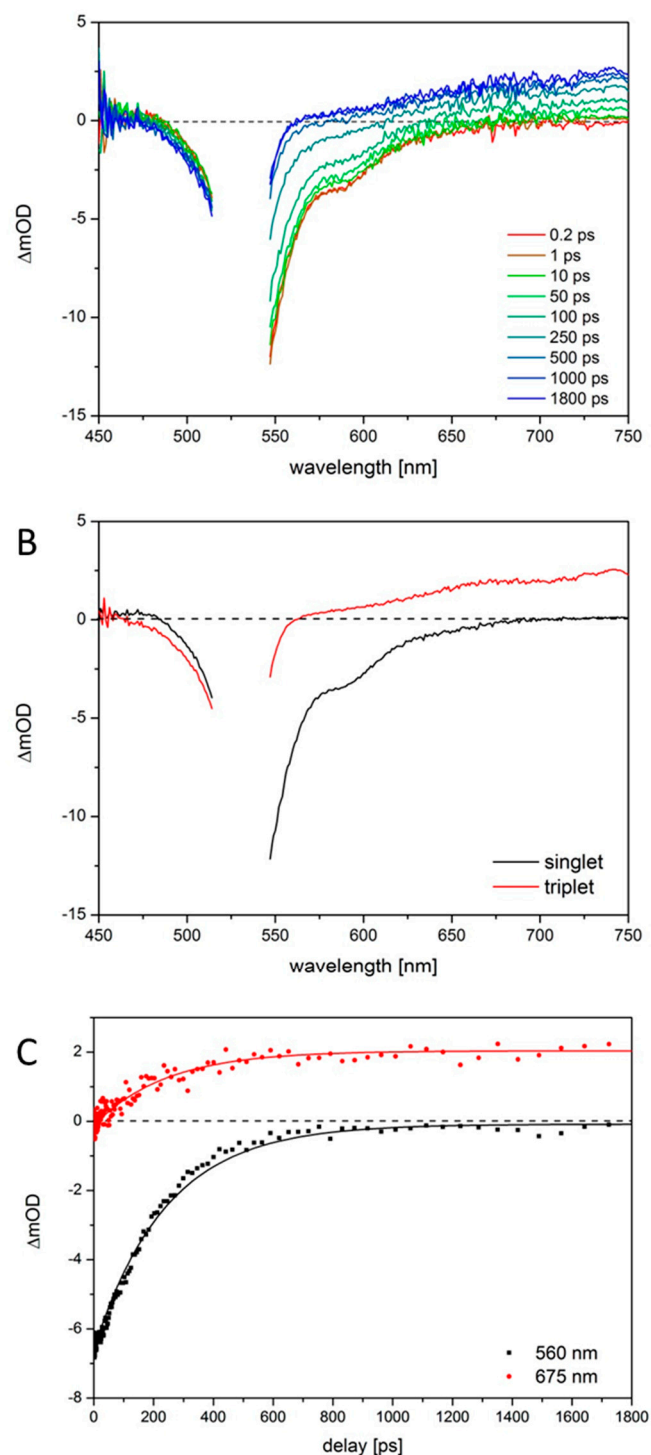


Figure S19. Formation of triplet state in 6: (A) transient spectra at selected delay times, (B) species spectra resulting from the global fit of the data, the spectrum of the initially populated species is assigned to the singlet state and contains mainly contributions of ground-state bleach and stimulated emission, the spectrum of the subsequently with a time constant of 240 ps populated species agrees well with the spectrum of the long-lived species in ns time-resolved measurements, which is assigned to the triplet state (C) kinetic traces at chosen probe wavelengths (line fits). The spectral region around the excitation wavelength (530 nm) was neglected in data evaluation due to a scattered pump.

ESI-MS Data

Table S1. ESI MS data of BODIPY dyes before and after photolysis ($\lambda > 420$ nm) of multicomponent catalyst systems with BODIPY dyes as PS, [Pd(PPh₃)Cl₂]₂ as WRC and TEA as SA in THF/H₂O (11:3) at $T = 25^\circ \text{C}$.

BODIPY dye	ESI MS of the pure dye	ESI MS after reaction	Comment
1	$m/z =$ no fragments could be assigned yet	$m/z = 266.21$ (M-Cl+5H) ⁺	Hydrogenated fragment
2	$m/z = 285.13$ (M+Na) ⁺ 263.15 (M+H) ⁺ 243.15 (M-F) ⁺	$m/z = 215.16$ (M-BF ₂ +2H) ⁺ 235.14 (M-2F+11H) ⁺	Hydrogenated fragments
3	$m/z = 512.93$ (M-H) ⁻	$m/z =$ no fragments could be assigned yet	
4	$m/z = 319.22$ (M-BF ₂ +H) ⁺	$m/z = 319.22$ (M-BF ₂ +H) ⁺	
5	$m/z = 515.09$ (M+Na) ⁺ 493.11 (M+H) ⁺ 473.10 (M-BF ₂) ⁺	$m/z = 319.22$ (M-I-BF ₂ +H) ⁺	Iodine free fragment
6	$m/z = 616.99$ (M-H) ⁻	$m/z = 319.22$ (M-2I-BF ₂ +H) ⁺	Iodine free fragment